

Supporting Information

P(VDF-TrFE) with High Molecular Entanglement for Enhanced Performance of Solid-State Lithium Batteries

Hanghua Wu,^{a,#} Shuangfeng Li,^{a,#} Weiwei Zhu,^b Jie Zhang,^c Baohui Ren^{a,} and Yan-Fei Huang^{a,*}, Zhong-Ming Li^{d,e}*

^a Guangdong Provincial Key Laboratory of New Energy Materials Service Safety, Shenzhen Key Laboratory of Polymer Science and Technology, College of Materials Science and Engineering Shenzhen University, Shenzhen 518055, P. R. China.

^b Zhejiang Chemical Industry Research Institute Co., Ltd, Hangzhou, 310023, China.

^c College of Polymer Science and Engineering and State Key Laboratory of Polymer Materials Engineering, Sichuan University, Chengdu 610065, P. R. China.

^d West China Hospital/West China School of Medicine, Sichuan University, Chengdu 610041, China

^e State Key Laboratory of Advanced Polymer Materials, Sichuan University, Chengdu 610065, China

These authors contribute equally to this work

* Corresponding author: yanfeihuang@szu.edu.cn; renbaohui@szu.edu.cn

Experimental Section

Materials

Poly(vinylidene fluoride-trifluoroethylene) (PVDF-TrFE, VDF/TrFE = 77.5/22.5, M_n = ~2374,000 g mol⁻¹、1032,000 g mol⁻¹、607,000 g mol⁻¹、491,000 g mol⁻¹) was kindly provided by Sinochem Lantian Co., Ltd. N, N-dimethylformamide (DMF, >99.9%). N-methyl-2-pyrrolidone (NMP, > 99.9%) was purchased from Aladin. LiFSI (99.9%), Super P Conductive Carbon Black (Super P), LiNi_{0.8}Co_{0.1}Mn_{0.1}O₂ (NCM811) and Li disks were supplied by Guangdong Canrd New Energy Technology Co., Ltd., China.

Synthesis of P(VDF-TrFE)

All P(VDF-TrFE) samples were synthesized via suspension free radical copolymerization of VDF and TrFE. The specific steps are as follows: a solution of deionized water (3000 g) and hydroxypropylmethyl cellulose stabilizer (1.5 g) was purged into a 5 L reactor containing at room temperature, after vacuum and N₂ refill four times, a mixture of VDF and TrFE monomer (1500 g, composition in mol%: 77.5/22.5) was purged. The reactor was heated to 55 °C with internal pressure regulated between 70 and 90 bar before the free radical initiator diisopropyl peroxydicarbonate (~25 g, 15 wt%) and chain transfer agent ethyl acetate (15–20 g) was introduced. After the pressure inside the reactor was run down below 40 bar, the polymerization was stopped by fast cooling the reactor to 10 °C. The crude product after venting was filtered, and the resulting fine white powder was washed eight times with deionized water at 60 °C (each wash lasting 1h). The final product was placed in a ventilated oven and dried at 80 °C for 24 h (yield >90wt%). The molecular weight and distribution of resulting polymer samples were controlled by the composition and addition protocol of initiator, monomer pressure, and chain transfer agent.

Preparation of Solid-state polymer electrolytes (SPEs)

The P(VDF-TrFE)-2.37 M SPE film was prepared via a solution casting method with a P(VDF-TrFE)-2.37 M : LiFSI weight ratio of 1 : 1, using DMF as solvents under magnetic stirring for 8 hours at 25 °C. Then, the polymer solution was poured into a glass petri dish and dried in an oven at 55 °C for ~24 hours before use. Other SPEs with different molecular weights were prepared under the same conditions.

Preparation of Cells

A slurry of NCM811, Super P, PVDF, and LiFSI with weight ratio 8 : 1 : 1 : 1 was magnetically stirred in NMP at 25 °C. The NCM811 cathode was prepared by casting the slurry onto aluminum foil and drying at 80 °C for 8 h, and the mass loading is around 1 mg cm⁻². P(VDF-

TrFE)-2.37 M w solid-state cells were assembled using a Li disk as an anode, NCM811 as cathode, or Li disks as both cathodes and anodes, with P(VDF-TrFE)-2.37 M as electrolyte in an argon-filled glove box. P(VDF-TrFE)-2.37 M SPE were sandwiched between two stainless steel (SS) plates, or a Li disk and a SS plate to obtain SS/P(VDF-TrFE)-2.37 M SPE/SS symmetrical cell or Li/P(VDF-TrFE)-2.37 M SPE/SS cell. Other cells were prepared under the same conditions with SPEs with different molecular weights.

Characterizations

The differential scanning calorimetry (DSC) measurements were carried out in an N₂ atmosphere with a temperature range of -50 to 200 °C and the ramping rate of 10 °C min⁻¹. Scanning electron microscopy (SEM) was used to examine the morphology of the electrolyte. The cross-sectional SEM images of the electrolyte were obtained after the sample was freeze-broken in liquid nitrogen. Fourier transform infrared (FTIR) measurements were used to determine the conformational changes of the polymer and the state of the residual solvent in the electrolyte. The samples were set in reflectance mode with a resolution of 8 cm⁻¹, a scan number of 96, and a scan range of 3200–400 cm⁻¹. X-ray diffractometer (XRD) was used to investigate the crystallinity and crystal structure of the samples, using Cu-K α radiation at a wavelength λ of 1.5418 Å. The mechanical properties of the electrolytes were measured by an electronic tensile machine at a tensile speed of 50 mm/min. Thermogravimetric analyzer (TGA) was carried out on the samples heated from room temperature to 800 °C under an N₂ atmosphere at a heating rate of 10 °C min⁻¹. Raman spectroscopy analysis was performed by scanning three times in confocal mode (laser intensity set to 50, scanning range from 1000 cm⁻¹ to 500 cm⁻¹), and peaks in the wave number range of 700 cm⁻¹ to 800 cm⁻¹ were fitted. The broadband dielectric spectroscopy (BDS) test was performed by placing the samples in a gold-spraying apparatus to perform a specific area of gold plating on the upper and lower surfaces using a circular aperture mold with a gold-sprayed area of 28.27 mm² (amplitude of 1.0 V applied voltage, frequency from 10⁷–10⁰ Hz). The coercive electric field and the residual polarization were obtained by obtaining the hysteresis return line of the samples through a ferroelectric tester. The upper and lower surfaces of the polymer matrix samples without lithium salts were gold-sprayed over an area of 28.27 mm². Tests were carried out at room temperature by applying a bipolar polarization electric field with a sine function (electric field strength 100–200 MV m⁻¹, frequency 10 Hz). The entanglement number (Z) was calculated from the following equations,

$$Z = \frac{M_w}{M_e} \quad (1)$$

$$M_e = \frac{\rho RT}{G_N^0} \quad (2)$$

where M_w is the average molecular weight, M_e is the molecular weight of entanglement, G_N^0 is the platform modulus, ρ is the density, R is the ideal gas constant, and T is the thermodynamic temperature. Small-amplitude oscillatory shear (SAOS) measurement was conducted at 180 °C, 200 °C, 220 °C, 240 °C and Time-temperature superposition (TTS) principle was used to obtain more reasonable G_N^0 from the platform portion of the storage modulus. The master curves of P(VDF-TrFE) at the reference temperature of 200 °C fitted by TTS principle and the results can be quantitatively analyzed by Eq. 1 and Eq. 2. For the density functional theory (DFT) calculation, Vienna *Ab initio* Simulation Package (VASP) is performed^[S1]. The generalized gradient approximation (GGA) with PBE is applied to the exchange correlation functional. DFT-D3 correction is used to account for the van der Waals interaction^[S2, S3]. The plane-wave cutoff energy is set to 500 eV and a Gamma k -mesh is utilized for Brillouin-zone integration. The convergence criteria are set to 10^{-5} eV for the energy and 0.02 eV Å⁻¹ for the maximal residual force. In each model a vacuum of 15 Å thickness is adopted for ensuring there is no interaction between periodic cells in each direction.

The adsorption energy between PVDF-TrFE molecules E_{ad1} is calculated by:

$$E_{ad1} = E_{2mol} - 2 \times E_{mol}$$

where E_{2mol} , and E_{mol} are the total energies of two PVDF-TrFE molecules and single PVDF-TrFE molecule.

The adsorption energy of Li on PVDF-TrFE molecules E_{ad2} is calculated by:

$$E_{ad2} = E_{tot} - E_{sub} - E_{Li}$$

Where E_{tot} and E_{sub} are the total energies with and without Li adsorption, and E_{Li} is the total energy of one Li atom.

Electrochemical Measurements

The impedance of various types of batteries was tested using EIS by applying sinusoidal AC signals with an amplitude of 10 mV (vs Ref) in the frequency range from 7 MHz to 1 Hz to obtain the impedance of various types of batteries at different frequencies. The ionic conductivity of electrolytes was tested using steel sheet symmetric cells placed in a thermostat oven and the temperature was increased from 25 °C to 80 °C, the thermostat was maintained at

10 °C intervals for 1 h and the cells were subjected to the EIS test after further thermostatzation.

The ionic conductivity was obtained by the formula:

$$\sigma = \frac{R}{LS}$$

where L is the electrolyte thickness, R is the impedance of the steel sheet symmetric cell and S is the area of the steel sheet. The migration activation energy E_a was obtained according to the Arrhenius formula:

$$\sigma = \sigma_0 \exp\left(-\frac{E_a}{RT}\right)$$

where σ_0 is the pre-exponential factor. Li/SPEs/Li cells were assembled and EIS measurements before and after polarization were performed at 10 mV amplitude in the range of 7 MHz to 1 Hz. t_{Li^+} is calculated based on the following equation:

$$t_{Li^+} = \frac{I_S(\Delta V - I_0 R_0)}{I_0(\Delta V - I_S R_S)}$$

where I_S and I_0 are the steady state and initial currents, respectively, and R_0 and R_S are the interface resistances before and after polarization.

The electrochemical window of the electrolyte was determined for Li/electrolyte/steel sheet cells at a scan rate of 1 mV s⁻¹ over the range of open-circuit E_{oc} to 6 V (vs. Ref).

Tests were also conducted to determine the critical current density (CCD) of the electrolyte by gradually increasing the current density of Li symmetric cells. Cyclic voltammetry (CV) tests were performed using NCM811//Li full cells at a scan rate of 0.2 mV s⁻¹ with 6 scans. The Li//Cu cells were tested to obtain Coulombic efficiency (CE) of the corresponding SPEs. A Li reservoir of 0.25 mAh cm⁻² was first deposited onto the Cu foil, followed by 10 subsequent cycles of plating and stripping at 0.05 mA cm⁻² for 0.05 mAh cm⁻² and the final exhaustive strip of the remaining Li reservoir was performed to the 1 V. The Li//Li symmetric cells were tested by charging and discharging at 25 °C with current densities of 0.1–0.3 mA cm⁻² (1 h per charging/discharging cycle) to obtain parameters such as cycle time and polarization voltage. In addition, the full cell assembled from NCM811 cathode was cycle tested at 25 °C in the voltage range of 2.8–4.3 V and at the charge/discharge rate of 0.05–5 C. The parameters such as Coulombic efficiency, specific capacity of discharge, charge/discharge plateau, cycling performance, and multiplicative performance were obtained.

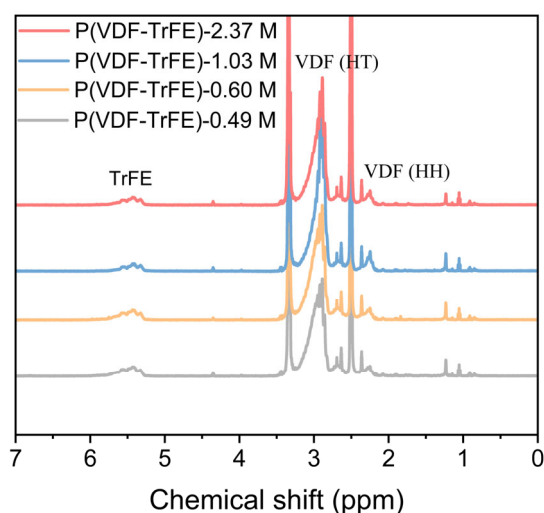


Figure S1. The ^1H NMR spectra of different molecular weights of the P(VDF-TrFE) sample. DMSO- d_6 was used as the solvent.

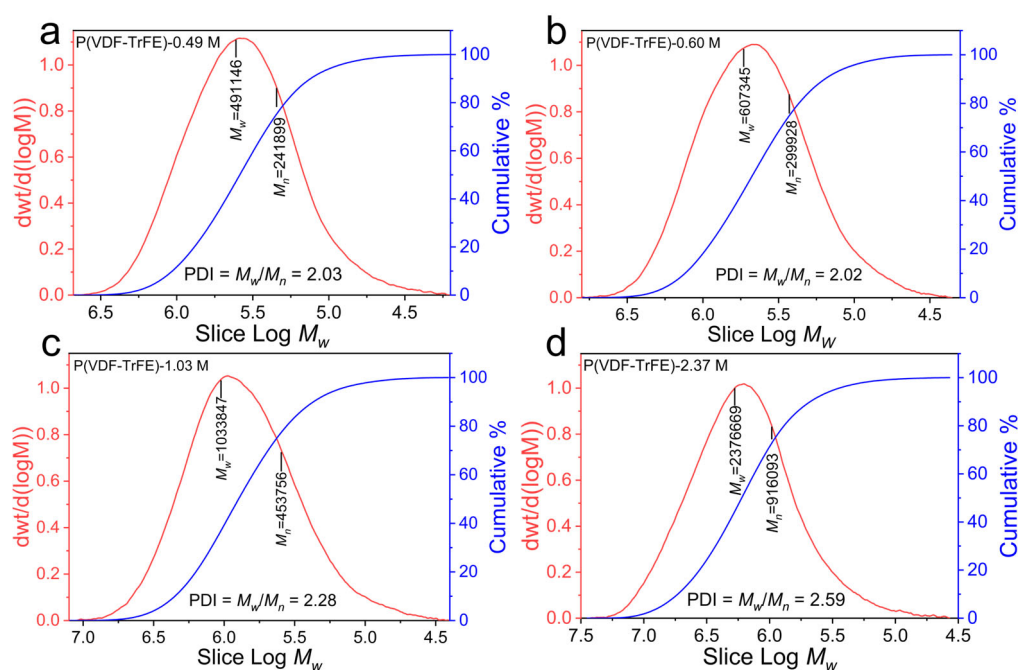


Figure S2. GPC molecular weight distribution curves of (a) P(VDF-TrFE)-0.49 M, (b) P(VDF-TrFE)-0.60 M, (c) P(VDF-TrFE)-1.03 M, and (d) P(VDF-TrFE)-2.37 M.

Table S1. The M_w , M_n , and PDI of P(VDF-TrFE)-0.49 M, P(VDF-TrFE)-0.60 M, P(VDF-TrFE)-1.03 M, and P(VDF-TrFE)-2.37 M.

Samples	M_n (g mol $^{-1}$)	M_w (g mol $^{-1}$)	PDI
P(VDF-TrFE)-0.49 M	241899	491146	2.03

P(VDF-TrFE)-0.60 M	299928	607345	2.02
P(VDF-TrFE)-1.03 M	453756	1033847	2.28
P(VDF-TrFE)-2.37 M	916093	2376669	2.59

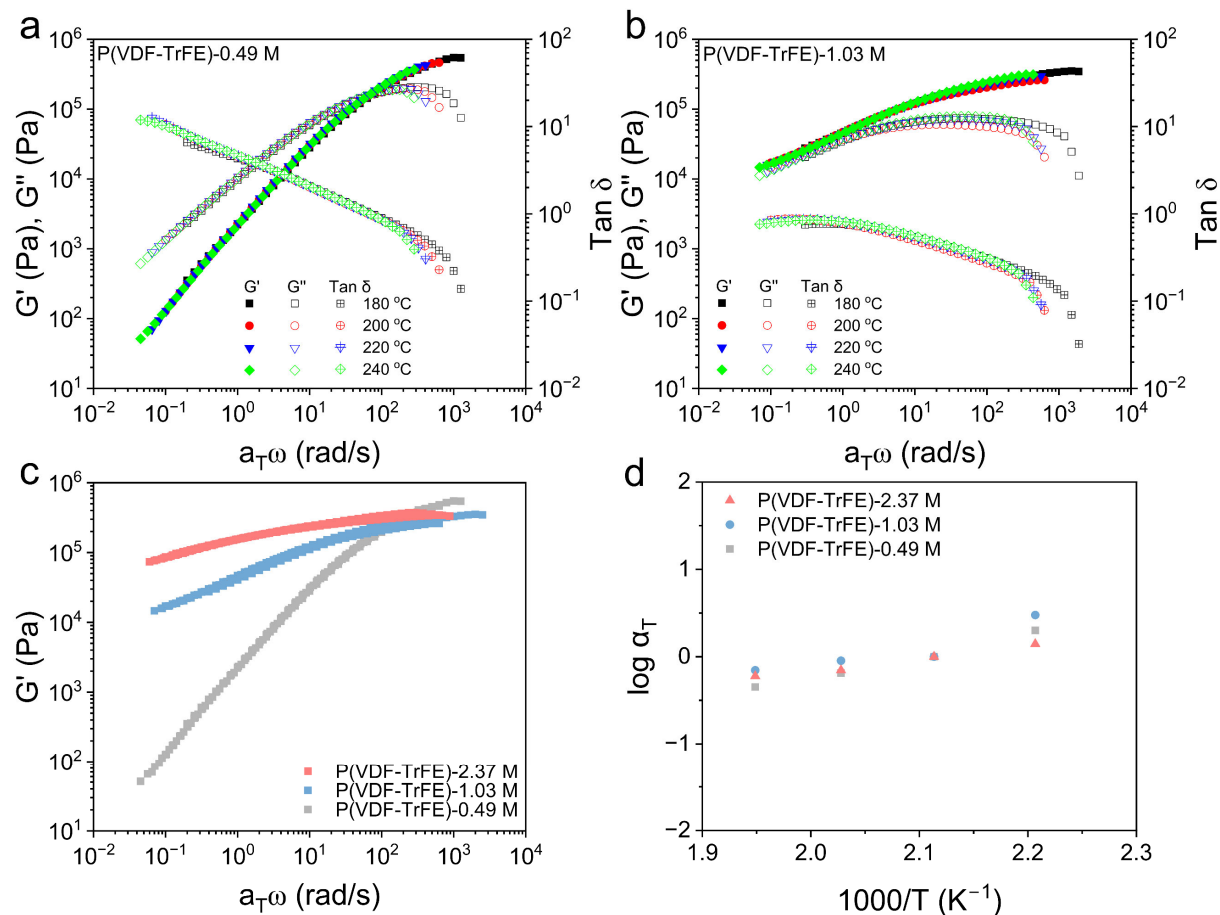


Figure S3. Curves of G' , G'' and $\tan \delta$ as a function of frequency for (a) P(VDF-TrFE)-0.49 M and (b) P(VDF-TrFE)-1.03 M. (c) Main curves of the P(VDF-TrFE) series after superposition of time and temperature. (d) TTS shift factors obtained for the P(VDF-TrFE) with varying molecular weights using a reference temperature of 200 °C

The energy storage modulus gradually increases with increasing shear frequency and a plateau region appears (Figure S3), noting that the energy storage modulus of P(VDF-TrFE)-2.37 M is always larger than the loss modulus, and the energy is mainly stored by elastic deformation rather than dissipated by viscous flow. In addition, it is observed that the corresponding frequency of the intersection of $G'=G''$ is gradually shifted to the lower frequency region (longer relaxation time) with the increase of molecular weight, and it is hypothesized that the intersection frequency of P(VDF-TrFE)-2.37 M exists at a lower frequency (<0.1 rad/s),

and the above results suggest that P(VDF-TrFE)-2.37 M has a stronger elasticity of the molecular chain and entanglement.

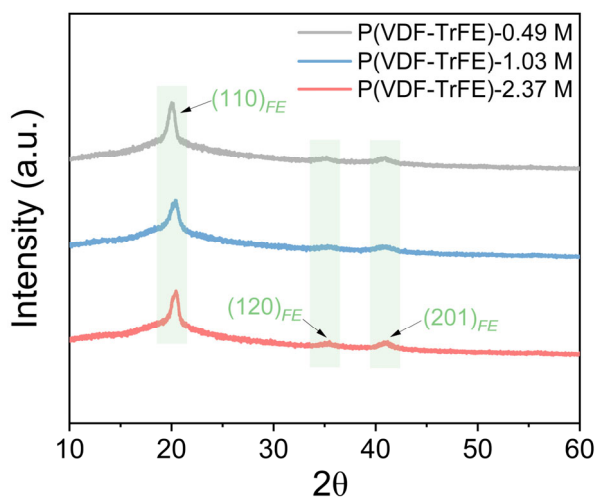


Figure S4. The XRD patterns of P(VDF-TrFE) electrolytes with different molecular weights.

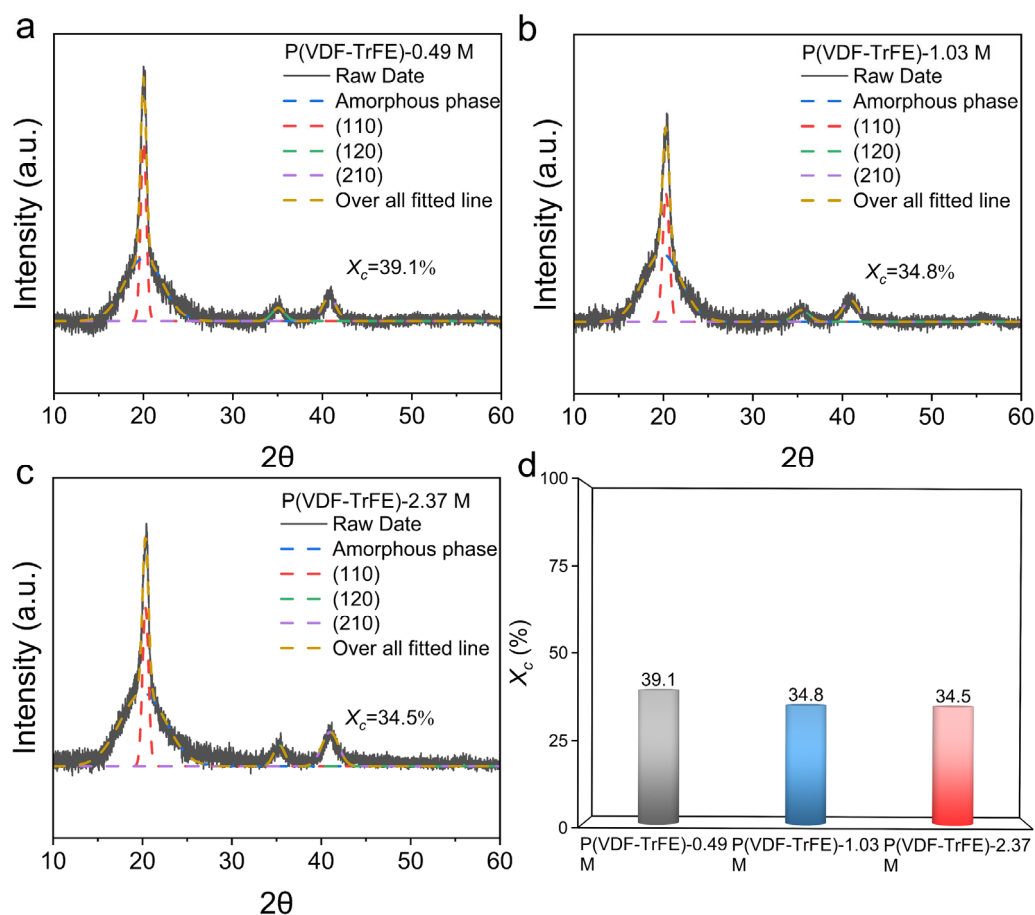


Figure S5. XRD peak fitting plot of (a) P(VDF-TrFE)-0.49 M SPE, (b) P(VDF-TrFE)-1.03 M SPE, and (c) P(VDF-TrFE)-2.37 M SPE. (d) The crystallinity of P(VDF-TrFE) SPEs.

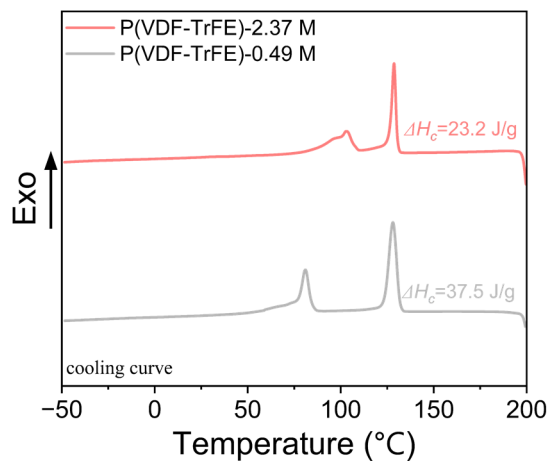


Figure S6. DSC cooling curve of P(VDF-TrFE) with different molecular weights.

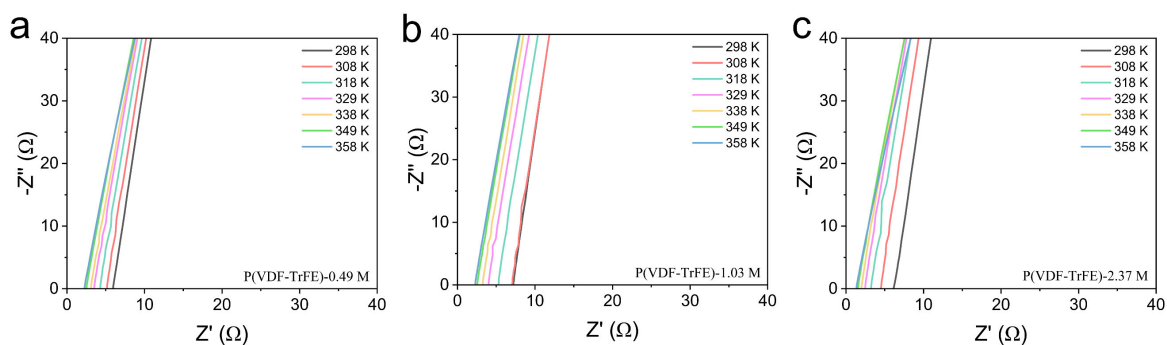


Figure S7. EIS curves of (a) P(VDF-TrFE)-0.49 M SPE, (b) P(VDF-TrFE)-1.03 M SPE, (c) P(VDF-TrFE)-2.37 M SPE withed by two stainless plates SS at varying temperatures.

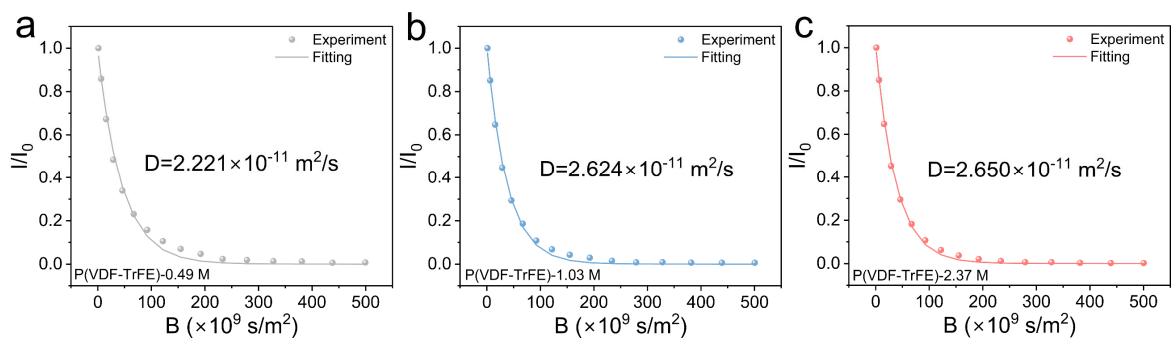


Figure S8. Li⁺ diffusion curves from PFG-NMR of (a) P(VDF-TrFE)-0.49 M, (b) P(VDF-TrFE)-1.03 M, and (c) P(VDF-TrFE)-2.37 M.

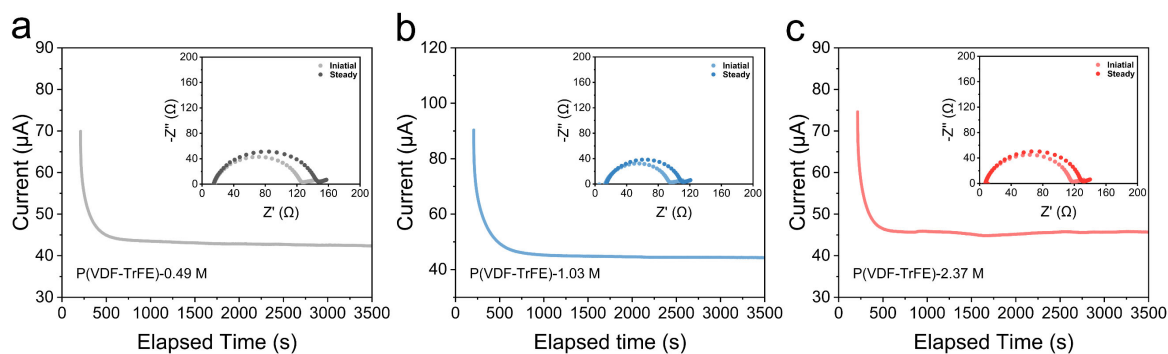


Figure S9. Chronoamperometry profiles of Li//Li symmetrical cells of (a) P(VDF-TrFE)-0.49 M, (b) P(VDF-TrFE)-1.03 M, (c) P(VDF-TrFE)-2.37 M. The insets show EIS curves before and after the polarization.

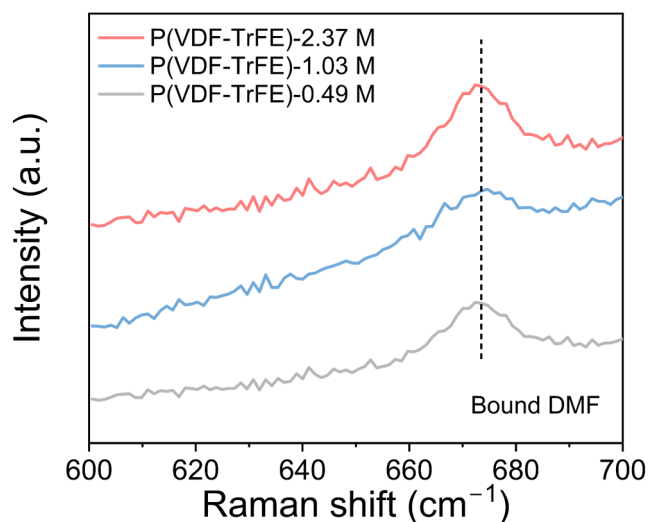


Figure S10. Raman spectroscopy in the range of 600–700 cm^{-1} of P(VDF-TrFE) with different molecular weight.

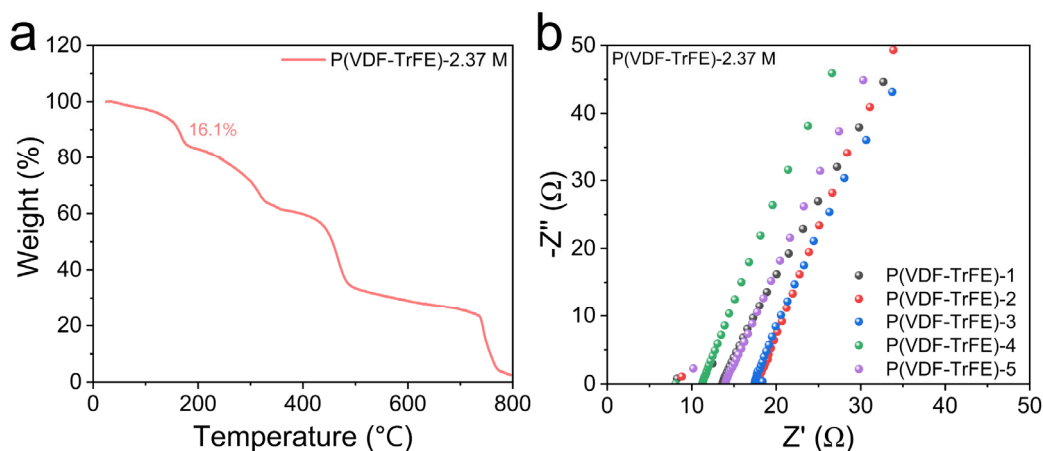


Figure S11. (a) Thermogravimetric analysis and (b) EIS curve of P(VDF-TrFE)-2.37 M .

Table S2. The ionic conductivity of P(VDF-TrFE)-2.37 M SPEs at room temperature.

Sample name	Film thickness (μm)	Impedance (Ω)	Ionic conductivity (S cm^{-1})
P(VDF-TrFE)-2.37M-1	0.111	13.4	4.23×10^{-4}
P(VDF-TrFE)-2.37M-2	0.105	13.7	3.91×10^{-4}
P(VDF-TrFE)-2.37M-3	0.114	17.8	3.26×10^{-4}
P(VDF-TrFE)-2.37M-4	0.104	10.8	4.92×10^{-4}
P(VDF-TrFE)-2.37M-5	0.126	17.1	3.75×10^{-4}

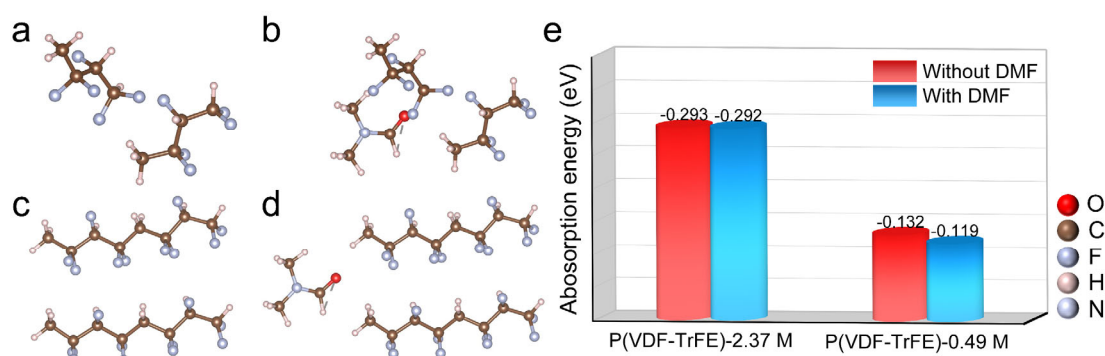


Figure S12. DFT calculation of the interchain adsorption energy on P(VDF-TrFE)-0.49 M (a) without DMF and (b) with DMF; P(VDF-TrFE)-2.37 M (c) without DMF and (d) with DMF. (e) The average adsorption energy of Li^+ obtained from a-d.

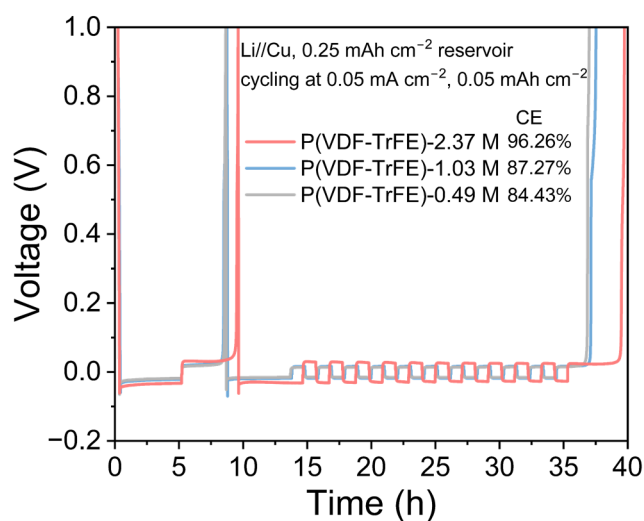


Figure S13. The CE of P(VDF-TrFE) SPEs with different molecular weight. A Li reservoir of 0.25 mAh cm^{-2} was first deposited onto the Cu foil, followed by 10 subsequent cycles of plating and stripping at 0.05 mA cm^{-2} for 0.05 mAh cm^{-2} . The final exhaustive strip of the remaining

Li reservoir was performed to the cut-off voltage, and the total capacity recovered was divided by the amount deposited to obtain the CE.

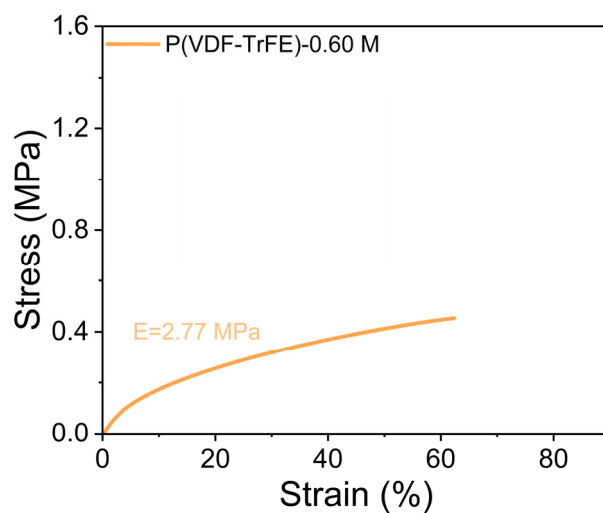


Figure S14. Stress-strain curve of P(VDF-TrFE)-0.60 M electrolytes.

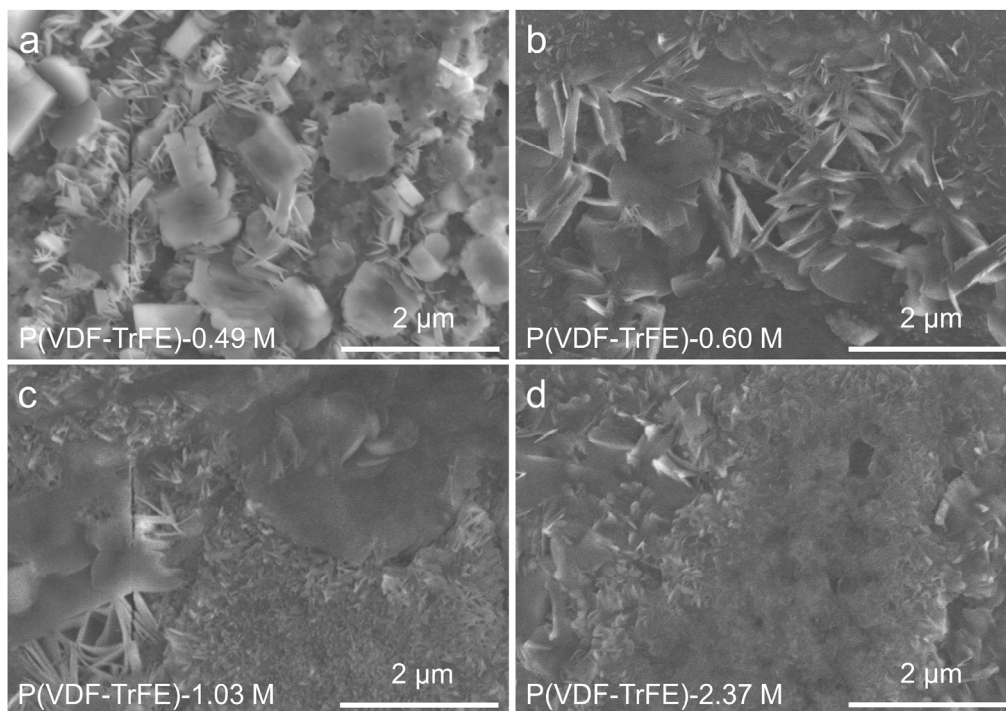


Figure S15. SEM images of the cycled Li surface from Li/P(VDF-TrFE) SPEs/Li symmetrical cells at current densities of 0.1 mA cm^{-2} .

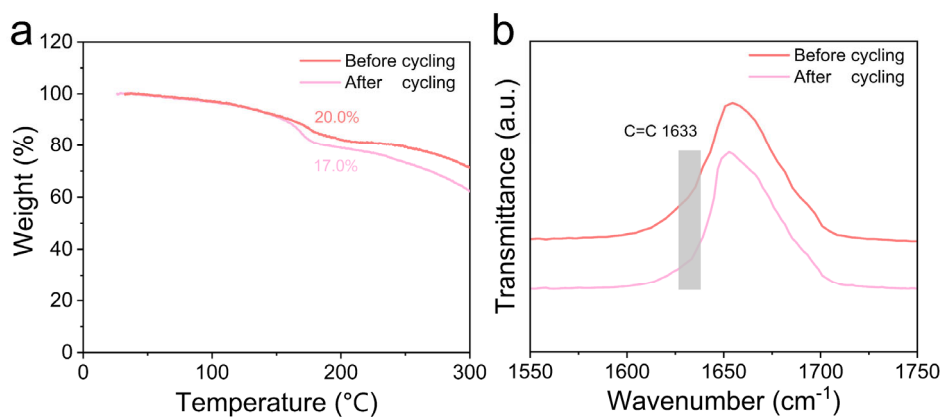


Figure S16. (a) TGA and (b) FTIR of P(VDF-TrFE)-2.37 M SPE of Li//Cu cells before and after cycling.

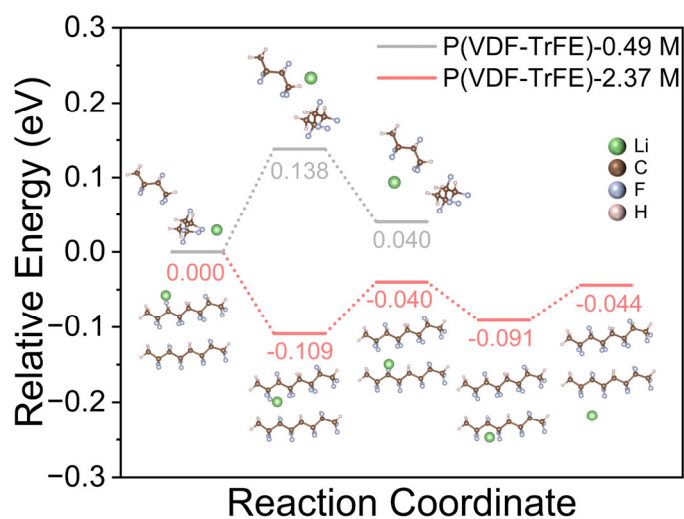


Figure S17. Profile of Li⁺ transport interchain, provided by DFT calculation.

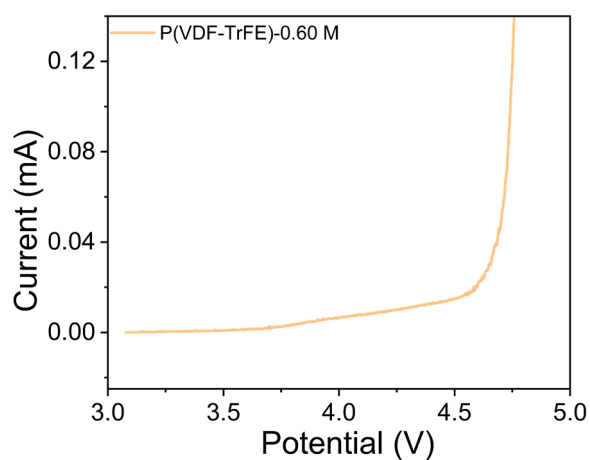


Figure S18. LSV curves of P(VDF-TrFE)-0.60 M SPEs at 25 °C.

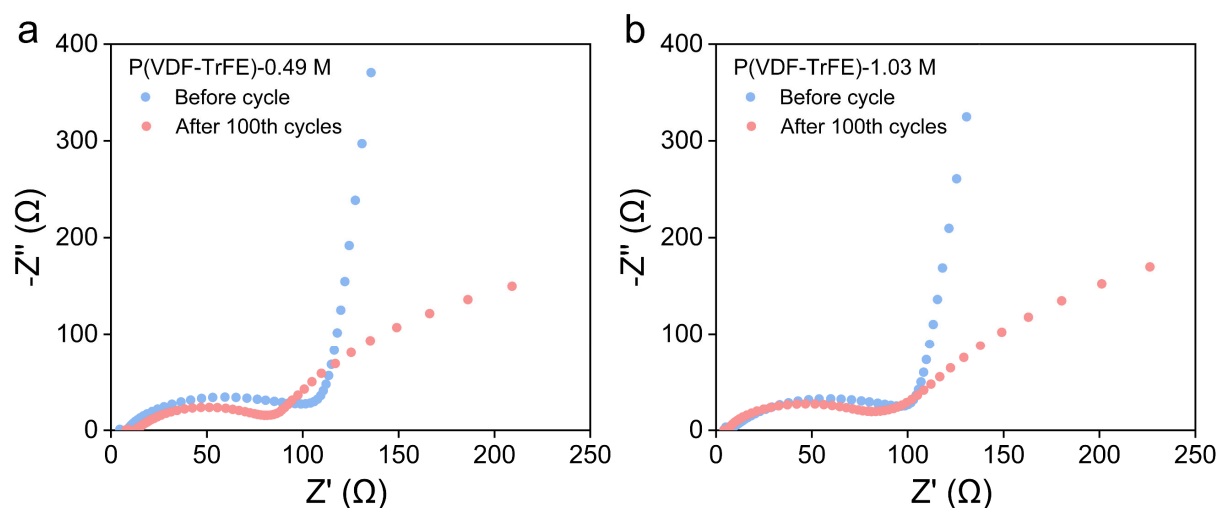


Figure S19. EIS test of the batteries before and after 100 cycles of (a) P(VDF-TrFE)-0.49 M, (b) P(VDF-TrFE)-0.60 M, and (c) P(VDF-TrFE)-1.03 M.

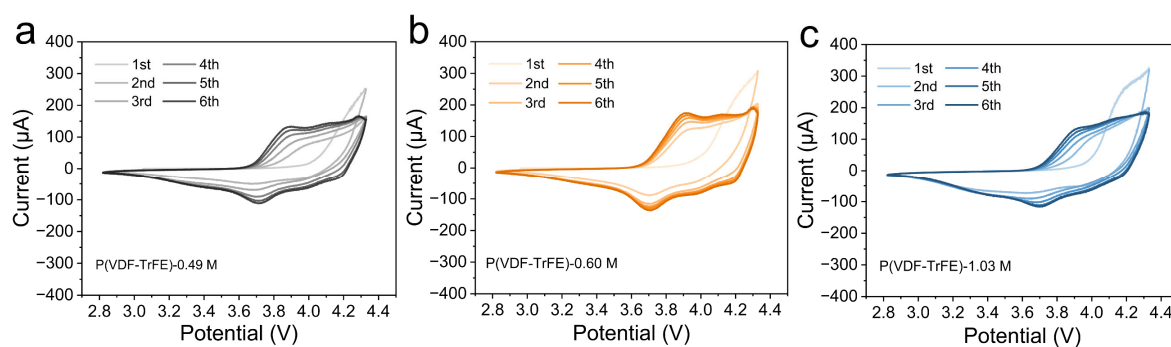


Figure S20. The CV curves of (a) P(VDF-TrFE)-0.49 M, (b) P(VDF-TrFE)-0.60 M, and (c) P(VDF-TrFE)-1.03 M.

References

- [S1] G. Kresse, D. Joubert, *Physical Review B* **1999**, 59, 1758-1775.
- [S2] S. Grimme, J. Antony, S. Ehrlich, H. Krieg, *The Journal of Chemical Physics* **2010**, 132, 154104.
- [S3] S. Grimme, S. Ehrlich, L. Goerigk, *J Comput Chem* **2011**, 32, 1456-1465.